



Article

Differential Expression of Subsets of Genes Related to HDL Metabolism and Atherogenesis in the Peripheral Blood in Coronary Artery Disease

Alexander D. Dergunov ^{1,*} , Elena V. Nosova ², Alexandra V. Rozhkova ², Margarita A. Vinogradina ², Veronika B. Baserova ¹, Mikhail A. Popov ³ , Svetlana A. Limborska ² and Liudmila V. Dergunova ²

¹ National Medical Research Center for Therapy and Preventive Medicine, Petroverigsky Street 10, Moscow 101990, Russia; veron1996@rambler.ru

² Laboratory of Human Molecular Genetics, National Research Center “Kurchatov Institute”, Kurchatov Sq. 2, Moscow 123182, Russia; el.nosova94@mail.ru (E.V.N.); avrojk@yandex.ru (A.V.R.); vin-rita@yandex.ru (M.A.V.); limbor.img@yandex.ru (S.A.L.); dergunova-lv.img@yandex.ru (L.V.D.)

³ Moscow Regional Research and Clinical Institute MONIKI, Moscow 129110, Russia; popovcardio88@mail.ru

* Correspondence: add1796@list.ru

Abstract: Differential expression of genes (DEGs) in coronary artery disease (CAD) and the association between transcript level and high-density lipoprotein cholesterol (HDL-C) were studied with 76 male patients with CAD and 63 control patients. The transcript level of genes related to HDL metabolism (24 genes) and atherosclerosis-prone (41 genes) in RNA isolated from peripheral blood mononuclear cells was measured by real-time RT-PCR. Twenty-eight DEGs were identified. The expression of cholesterol transporters, *ALB*, *APOA1*, and *LCAT* was down-regulated, while the expression of *AMN*, *APOE*, *LDLR*, *LPL*, *PLTP*, *PRKACA*, and *CETP* was up-regulated. The systemic inflammation in CAD is evidenced by the up-regulation of *IL1B*, *TLR8*, *CXCL5*, and *TNFRSF1A*. For the controls, *TLR8* and *SOAT1* were negative predictors of the HDL-C level. For CAD patients, *PRKACG*, *PRKCQ*, and *SREBF1* were positive predictors, while *PRKACB*, *LCAT*, and *S100A8* were negative predictors. For CAD patients, the efficiency of reverse cholesterol transport is 73–79%, and intracellular free cholesterol seems to accumulate at hyperalphalipoproteinemia. Both atheroprotective (via *S100A8*) and proatherogenic (via *SREBF1*, *LCAT*, *PRKACG*, *PRKACB*, and *PRKCQ*) associations of gene expression with HDL-C determine HDL functionality in CAD patients. The selected key genes and involved pathways may represent HDL-specific targets for the diagnosis and treatment of CAD and atherosclerosis.

Keywords: atherosclerosis; coronary artery disease; differentially expressed genes; HDL metabolism; inflammation; transcript



Citation: Dergunov, A.D.; Nosova, E.V.; Rozhkova, A.V.; Vinogradina, M.A.; Baserova, V.B.; Popov, M.A.; Limborska, S.A.; Dergunova, L.V. Differential Expression of Subsets of Genes Related to HDL Metabolism and Atherogenesis in the Peripheral Blood in Coronary Artery Disease. *Curr. Issues Mol. Biol.* **2023**, *45*, 6823–6841. <https://doi.org/10.3390/cimb45080431>

Academic Editor: Emiel P.C. van der Vorst

Received: 30 July 2023

Revised: 12 August 2023

Accepted: 14 August 2023

Published: 16 August 2023



Copyright: © 2023 by the authors. Licensee MDPI, Basel, Switzerland. This article is an open access article distributed under the terms and conditions of the Creative Commons Attribution (CC BY) license (<https://creativecommons.org/licenses/by/4.0/>).

1. Introduction

Coronary atherosclerosis and coronary heart disease (CAD) are characterized by disturbances of lipoprotein metabolism, innate and adaptive immunity, and inflammation. Myeloid cells acquire proinflammatory features that activate the cascade of signaling events associated with cholesteryl ester accumulation in macrophages [1,2]. Foam cell formation is influenced in part by the proatherogenic and antiatherogenic balances of LDL and HDL, respectively. The cholesterol stationary level in macrophages is maintained by tight control of cholesterol influx with LDL and cholesterol efflux to HDL via cholesterol transporters [3] as a first step in reverse cholesterol transport to the liver for cholesterol excretion. The cholesterol efflux capacity (CEC) of HDL determines its antiatherogenic effect rather than HDL cholesterol level [4]. However, recent findings have challenged the casual relationship between CEC and atherosclerosis [5–7], and this issue is actively debated [1].

ABCA1-mediated cholesterol efflux is an exclusive route to lipid-free apoA-I, whereas ABCG1 and scavenger receptor BI (SR-BI) are involved in cholesterol efflux to

HDL [8–10]. The second step includes the synthesis of cholesteryl ester (CE) molecules, which is catalyzed by lecithin:cholesterol acyltransferase (LCAT). The inclusion of hydrophobic CE molecules into the particle core results in the transition from discoidal to spherical shapes of HDL particles [11]. The third step includes the selective uptake of CE molecules from HDL particles by hepatocytes via SR-BI [12] (direct RCT) or the exchange of CE in HDL for triglycerides in LDL via the CE transfer protein (CETP). CE-enriched LDL particles bind to the LDL receptor in hepatocyte membranes and are internalized (indirect RCT). Modified LDL decreases the expression of SR-BI but induces the expression of SR-B [13]. The activity of the phospholipid-transfer protein (PLTP) induces the remodeling of large HDL particles with concomitant fusion–fission of these particles, which results in the regeneration of small HDL particles and the dissociation of lipid-free apoA-I [14].

The synthesis and uptake of triglyceride and cholesterol molecules are regulated by the sterol-regulatory element-binding proteins *SREBP1* and *SREBP2*, respectively. *SREBP1* increases fatty acid synthesis. Transcription of the *SREBP1c* gene is increased by insulin (an activator) and decreased by glucagon (an inhibitor) [15]. Transcription of the *SREBP1c* gene is also activated by liver X receptors (LXRs), thereby assuring a supply of fatty acids at sterol overloading to allow storage of excess cholesterol as cholesteryl ester [16]. LXR α (NR1H3) and LXR β (NR1H2) are members of the nuclear hormone receptor superfamily of ligand-dependent transcription factors that regulate transcription in response to the direct binding of cholesterol derivatives [17]. *SREBP2* acts through the increase of transcription of target genes for cholesterol synthesis or uptake through the LDL receptor at the decrease of cholesterol levels in the ER membrane. *SREBP1a* in mouse macrophages links lipid metabolism to the innate immune response [18,19]. However, inconsistent data exist on *SREBP*'s expression at CAD [20,21]. Another cholesterol sensor, HMG CoA reductase, a rate-limiting step in cholesterol synthesis, is rapidly degraded at cholesterol accumulation in ER membranes [22]. The cholesterol in macrophages is esterified by acyl coenzyme A:cholesterol acyltransferase 1 (SOAT1 aka ACAT1) and is regenerated from cholesteryl ester by neutral cholesteryl ester hydrolase [23]. Cholesterol influx through the LDL receptor and scavenger receptor CD36 for oxidized LDL, cholesterol efflux, cholesterol synthesis, and storage as cholesteryl ester determine the cholesterol pool level in the plasma membrane accessible for efflux [24].

The existence of various cell populations in atheroma is rapidly recognized based mainly on single-cell RNA sequencing [25]. It has been assumed that atherosclerotic arteries contain several macrophage subsets endowed with specific functions [26]. Also, foamy and non-foamy macrophages have been suggested to exist in atherosclerotic plaque and lipid-loaded plaque macrophages are not likely the plaque macrophages that drive lesional inflammation [27], thus contrasting with the promotion of macrophage foam cell formation, activation of the NLRP3 inflammasome, and atherogenesis at *Abca1/Abcg1* deficiency [28]. The non-coincident changes in pro-inflammatory gene expression in foam cells compared to non-foam cells may complicate the overall analysis of lesional inflammation. Moreover, HDL may possess both anti- and pro-inflammatory effects via cholesterol efflux [29] and Toll-like receptor-induced PKC signaling [30], respectively. Thus, it seems reasonable to perform a combined study of the expression of genes involved in lipid metabolism and inflammation in relation to HDL levels in CAD.

Based on the available data on differential expression genes at CAD established by RNA-seq and the analysis of genes involved in lipoprotein metabolism and atherogenesis, we recently suggested two pools of genes (HDL cluster and atherogen cluster, 64 genes total) to perform an analysis of the expression of these genes with a conventional real-time RT-PCR [31]. In the present study, the *SOAT1* gene was added to the HDL cluster to analyze the traffic of intracellular cholesterol. We used two gene pools: first, to reveal the differential expression of genes in the HDL cluster and atherogen cluster in peripheral blood mononuclear cells from CAD patients; second, to relate gene expression to the metabolic pathways involved in CAD; finally, to establish the significance of particular transcripts with proatherogenic or atheroprotective properties as predictors of HDL level both in

CAD and control patients in relation to HDL functionality. We collected blood samples from control and CAD patients unaffected by any previous lipid-lowering treatment to avoid any changes in lipid metabolism, immune status, or inflammation status induced by such treatment.

2. Materials and Methods

2.1. Patients and Laboratory Tests

One hundred thirty-nine Caucasian male subjects from Moscow and Moscow District, 40–60 years old, were divided into two cohorts. The first cohort ($n = 63$) included patients without coronary atherosclerosis, while the second one ($n = 76$) included patients with CAD and stenosis of coronary arteries verified by standard coronary angiography for each patient in the two cohorts. The hemodynamically significant stenosis was diagnosed in a case of more than 50% luminal narrowing in at least one vessel, and these patients were included in the CAD cohort. The patients without any visible stenosis or with hemodynamically insignificant (<20%) stenosis were included in the control cohort. All patients in the two cohorts were without hypertension or diabetes, not alcoholics, and not on treatment with corticosteroids or lipid-lowering drugs for at least 3 months before drawing a blood sample. The latter requirement originates from the known prominent changes in lipid metabolism induced by lipid-lowering therapy. To deal with unaffected blood samples, we searched for new patients without any previous hypolipidemic treatment, first by selecting patients with chest pain and with electrocardiogram and/or echocardiogram abnormalities at the stage of outpatient care, followed by coronary angiography to diagnose CAD, second by blood drawing, and, finally, by the beginning of adequate therapy, including lipid-lowering drugs. Written informed consent was obtained from each patient included in the study. The study protocol conforms to the ethical guidelines of the 1975 Declaration of Helsinki and has been approved by the local ethics committee for research on humans. The lipid profiles were determined enzymatically with commercial kits on an Architect c8000 autoanalyzer (Abbott, Abbott Park, IL, USA). Plasma apoA-I and apoB levels were measured with immunoturbidimetric kits from DiaSys (Holzheim, Germany) on a Sapphire 400 autoanalyzer (Hirose Electronic System, Tokyo, Japan).

2.2. Gene Expression Analysis by Real-Time RT-PCR

Ficoll-Hypaque (1.077 g/mL) density gradient centrifugation (Sigma, St. Louis, MO, USA) was performed to isolate peripheral blood mononuclear cells. Total RNA was isolated with TRI Reagent (Molecular Research Center, Cincinnati, OH, USA) and traces of DNA were removed by DNase I in the presence of an RNase inhibitor according to the manufacturer's protocol (ThermoFisher Scientific, Waltham, MA, USA). RNA samples were kept at -70°C . RNA concentration and quality (RQI > 9) were measured with the Experion electrophoresis system (Bio-Rad, Hercules, CA, USA). cDNA was synthesized with the RevertAid First Strand cDNA Synthesis Kit (ThermoFisher Scientific, Waltham, MA, USA), and cDNA samples were kept at -20°C .

The HDL cluster included the following twenty-four genes (Supplementary Table S1): Albumin (*ALB*); Alpha-2-macroglobulin (*A2M*); Amnion associated transmembrane protein (*AMN*); Apolipoprotein A1 (*APOA1*); Apolipoprotein E (*APOE*); ATP binding cassette subfamily A member 1 (*ABCA1*); ATP binding cassette subfamily A member 5 (*ABCA5*); ATP binding cassette subfamily G member 1 (*ABCG1*); Bone morphogenetic protein 1 (*BMP1*); Cholesteryl ester transfer protein (*CETP*); Cubilin (*CUBN*); High density lipoprotein binding protein (*HDLBP*); 3-hydroxy-3-methylglutaryl-CoA reductase (*HMGCR*); Lecithin-cholesterol acyltransferase (*LCAT*); Lipase C, hepatic type (*LIPC*); Lipoprotein lipase (*LPL*); Low density lipoprotein receptor (*LDLR*); Phospholipid transfer protein (*PLTP*); Protein kinase cAMP-activated catalytic subunit alpha (*PRKACA*); Protein kinase cAMP-activated catalytic subunit beta (*PRKACB*); Protein kinase cAMP-activated catalytic subunit gamma (*PRKACG*); Scavenger receptor class B member 1 (*SCARB1*); Sterol O-acyltransferase 1 (*SOAT1*); Zinc finger DHHC-type containing 8 (*ZDHHC8*).

The atherogen cluster included the following 41 genes (Supplementary Table S1): Asialoglycoprotein receptor 2 (*ASGR2*); CD14 molecule (*CD14*); CD36 molecule (*CD36*); Coagulation factor V (*F5*); Colony stimulating factor 1 receptor (*CSF1R*); Colony stimulating factor 2 receptor beta common subunit (*CSF2RB*); C-X-C motif chemokine ligand 5 (*CXCL5*); Cytochrome b-245 alpha chain (*CYBA*); Integrin subunit alpha 2b (*ITGA2B*); Integrin subunit alpha M (*ITGAM*); Integrin subunit beta 3 (*ITGB3*); Intercellular adhesion molecule 1 (*ICAM1*); Interleukin 1 beta (*IL1B*); Interleukin 1 receptor type 1 (*IL1R1*); Interleukin 18 (*IL18*); Interleukin 18 receptor 1 (*IL18R1*); Interleukin 18 receptor accessory protein (*IL18RAP*); Junctional adhesion molecule 3 (*JAM3*); Lymphotoxin alpha (*LTA*); Matrix metalloproteinase 9 (*MMP9*); Microsomal glutathione S-transferase 1 (*MGST1*); NPC intracellular cholesterol transporter 1 (*NPC1*); NPC intracellular cholesterol transporter 2 (*NPC2*); Nuclear receptor subfamily 1 group H member 2 (*NR1H2*); Nuclear receptor subfamily 1 group H member 3 (*NR1H3*); Oxidized low density lipoprotein receptor 1 (*OLR1*); Phosphatidylcholine transfer protein (*PCTP*); Phospholipase A2 group VII (*PLA2G7*); Protein kinase C theta (*PRKCQ*); S100 calcium binding protein A12 (*S100A12*); S100 calcium binding protein A8 (*S100A8*); S100 calcium binding protein A9 (*S100A9*); Secretory leukocyte peptidase inhibitor (*SLPI*); Solute carrier family 7 member 11 (*SLC7A11*); Sterol regulatory element binding transcription factor 1 (*SREBF1*); Superoxide dismutase 2 (*SOD2*); TNF receptor superfamily member 1A (*TNFRSF1A*); TNF receptor superfamily member 1B (*TNFRSF1B*); Toll like receptor 5 (*TLR5*); Toll like receptor 8 (*TLR8*); Vascular endothelial growth factor A (*VEGFA*).

Housekeeping genes included Glyceraldehyde-3-phosphate dehydrogenase (*GAPDH*), Lactate dehydrogenase A (*LDHA*), and Ribosomal protein L3 (*RPL3*) genes (Supplementary Table S1).

Gene-specific primers were designed using OLIGO Primer Analysis Software 6.31 (Molecular Biology Insights, Colorado Springs, CO, USA). Primer structures and coordinates are given in Supplementary Table S1. The specificity of the primers was verified by the melting curve of the PCR product (a single peak). Real-time RT-PCR (RT-PCR) was carried out on a StepOnePlus Real-Time PCR System (Applied Biosystems, Foster City, CA, USA) in 25 μ L of reaction mixture containing 2 μ L of 1:30 or 1:6 diluted cDNA, 5 pmol each of forward and reverse primers, and 5 μ L 5x PCRMix-HS SYBR (Evrogen, Moscow, Russia). The amplification protocol included: (1) a hot start at 95 °C for 10 min; (2) 40 cycles at 95 °C for 15 s, 65 °C for 25 s, and 72 °C for 35 s; data were collected at the elongation step; (3) melting curve was obtained by heating from 65 °C to 95 °C with a 0.3 °C step.

2.3. Interaction between Protein Products of Genes and Pathway Analyses

The differentially expressed genes were annotated by functional enrichment analysis with the Gene Ontology (GO) [32,33] and the Kyoto Encyclopedia of Genes and Genomes (KEGG) [34] pathway databases. The online tool Database for Annotation, Visualization, and Integrated Discovery (DAVID) [35] was explored to detect GO categories. The analysis of protein–protein interactions (PPI) was performed with the Search Tool for the Retrieval of Interacting Genes (STRING) database [36]. The data generated by the STRING database were visualized with Cytoscape [37] and KEGG pathway analysis was conducted with the Cytoscape functional enrichment module. The *p*-value for PPI enrichment is an indicator of interaction efficiency. The number of nodes and the number of edges are network characteristics.

2.4. Statistical Analysis

Statistica (version 13) software was used. The data are given as mean values with standard deviations. The Kolmogorov–Smirnov test was used to check the normality, and the variables with a skewed distribution were log-transformed. Differences in continuous variables between groups were analyzed by ANOVA with posteriori estimates by Fisher's LSD test or the Mann–Whitney test. The statistical significance limit was accepted as

$p < 0.05$. Pearson's correlation coefficients were calculated to describe relationships between variables. Multiple linear regression was performed as well. The cohort sizes were sufficient for the robust correlation and regression analyses at the $p = 0.05$ level, as verified by power and sample size analyses. In multiple regression, the assumption that the residuals (predicted minus observed values) are distributed normally was verified by a normal probability plot of residuals. Furthermore, the Darbin–Watson statistic DW was used as a test for checking autocorrelation in the residuals; no first-order autocorrelation was assumed for DW values 1.50–2.50. The multicollinearity of the predictors in the regression equation was checked by the value of the variance inflation factor (VIF), which is a reciprocal of tolerance. Tolerance for the i th independent variable is 1 minus, the proportion of variance it shares with the other independent variable in the analysis; this represents the proportion of variance in the i th independent variable that is not related to the other independent variables in the model. The VIF value of 1 corresponds to the complete absence of multicollinearity, and the generally accepted VIF values lower than 4 correspond to negligible multicollinearity and the accurate values of regression coefficients [38]. Paired analysis of RT-PCR data was conducted with the REST-2009 software [39], and the data are given as a mean value of expression ratio with the standard error as a 68% confidence interval. The permutation test used in the REST-2009 software is designed to determine whether the observed difference between the sample means is large enough to reject; at some significance level, the null hypothesis that the data drawn from the control is from the same distribution as the data drawn from the treatment group. The data verified by the permutation test are much more robust and do not require any previous knowledge of the nature of the distribution. In addition, the relative expression of all target genes normalized by the geometric mean of three reference genes [40] was used in the analysis. The false discovery rate (FDR) for multiple comparisons was controlled by the Benjamini–Hochberg procedure [41]. The FDR value was fixed at the 0.05 level unless indicated. The raw p -values significant under the Benjamini–Hochberg procedure are given in the analysis of gene expression.

3. Results

3.1. Lipid and Lipoprotein Levels and Anthropometric Data of the Patients

The number of patients in the control and CAD cohorts was equal to 63 and 76 patients, respectively. Age, body mass index (BMI), plasma lipoprotein, and apolipoprotein data for patients in two cohorts are included in Table 1. The mean values of total cholesterol, LDL-C, nonHDL-C, and atherogenicity index were lower in CAD compared to controls, while apoA-I and age were significantly higher. The cohorts did not differ from each other by HDL-C, VLDL-C, plasma TG, apoB, or BMI. Notably, cholesterol content in a single LDL particle, calculated from the mean levels of Chol, LDL-C, TG, and apoB, was 25% lower for CAD patients compared to controls.

Table 1. Laboratory and anthropometric parameters for two cohorts of patients. Mean \pm SD values and their comparison by Mann–Whitney test are included.

| | Control ($n = 63$) | CAD ($n = 76$) | p |
|------------------------|----------------------|---------------------|-------|
| HDL-C, mM | 1.25 \pm 0.43 | 1.21 \pm 0.57 | 0.133 |
| Chol, mM | 5.04 \pm 1.28 | 4.21 \pm 1.32 & | 0.000 |
| LDL-C, mM | 3.08 \pm 1.04 | 2.32 \pm 0.97 & | 0.000 |
| VLDL-C, mM | 0.72 \pm 0.34 | 0.68 \pm 0.31 | 0.559 |
| nonHDL-C, mM | 3.79 \pm 1.10 | 3.00 \pm 1.04 & | 0.000 |
| TG, mM | 1.55 \pm 0.74 | 1.48 \pm 0.68 | 0.697 |
| atherogenicity index | 3.32 \pm 1.25 | 2.87 \pm 1.40 & | 0.017 |
| apoA-I, mg/dL | 140.51 \pm 38.19 | 157.83 \pm 48.7 & | 0.027 |
| apoB, mg/dL | 87.32 \pm 20.67 | 84.27 \pm 25.37 | 0.259 |
| BMI, kg/m ² | 28.63 \pm 2.75 | 28.14 \pm 3.57 | 0.599 |
| age, year | 49.05 \pm 5.63 | 54.07 \pm 4.18 & | 0.000 |

& significant difference between CAD and control cohorts ($p < 0.05$).

3.2. Expression of Genes Related to HDL Metabolism and Atherogenesis in Control and CAD Cohorts

3.2.1. Differential Gene Expression

The transcript levels of genes related to HDL metabolism (HDL cluster) and atherogenesis (atherogen cluster) selected by us earlier [31,42] were measured by real-time RT-PCR. The *SOAT1* gene was additionally included in the HDL cluster to follow the intracellular cholesterol traffic. The differential expression at the transcript level in CAD versus control cohorts (fold change) was analyzed with the REST-2009 software. The multiple comparisons were controlled with the Benjamini–Hochberg procedure with an FDR value of 0.05.

A total of 28 DEGs in CAD were identified by the REST, and the data are given in Figure 1. Compared with control, seven genes in the HDL cluster—amion-associated transmembrane protein (*AMN*), apolipoprotein E (*APOE*), cholesteryl ester transfer protein (*CETP*), low density lipoprotein receptor (*LDLR*), lipoprotein lipase (*LPL*), phospholipid transfer protein (*PLTP*), and protein kinase cAMP-activated catalytic subunit alpha (*PRKACA*)—were up-regulated, and six genes, namely, ATP binding cassette subfamily A member 1 (*ABCA1*), ATP binding cassette subfamily A member 5 (*ABCA5*), albumin (*ALB*), apolipoprotein A1 (*APOA1*), lecithin-cholesterol acyltransferase (*LCAT*), and scavenger receptor class B member 1 (*SCARB1*), were down-regulated in CAD.

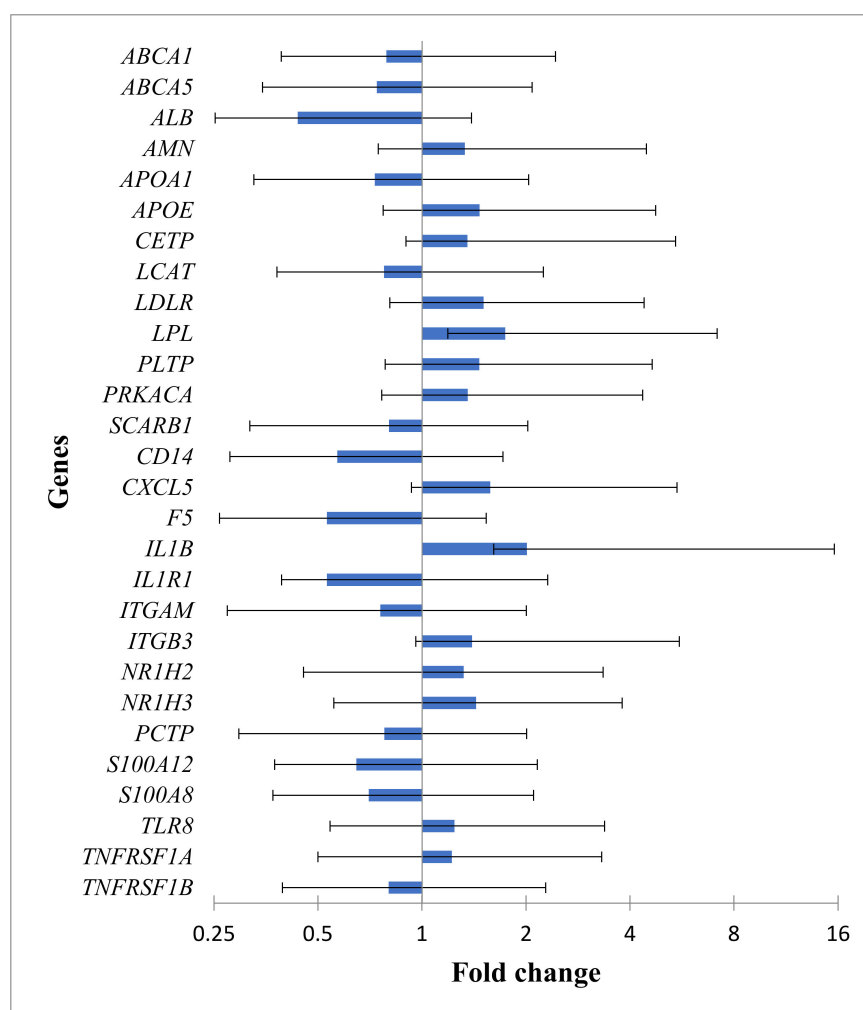


Figure 1. The change of gene expression in two gene clusters in CAD. The fold change for HDL and atherogen clusters was calculated with the REST-2009 software. Only significant changes controlled for multiple comparisons by the Benjamini–Hochberg procedure (FDR = 0.05) are given as mean (SE) values.

Analogously, seven genes in the atherogen cluster—C-X-C motif chemokine ligand 5 (*CXCL5*), interleukin 1 beta (*IL1B*), integrin subunit beta 3 (*ITGB3*), nuclear receptor subfamily 1 group H member 2 (*NR1H2*), nuclear receptor subfamily 1 group H member 3 (*NR1H3*), Toll-like receptor 8 (*TLR8*), and TNF receptor superfamily member 1A (*TNFRSF1A*)—were up-regulated, and eight genes—CD14 molecule (*CD14*), coagulation factor V (*F5*), interleukin 1 receptor type 1 (*IL1R1*), integrin subunit alpha M (*ITGAM*), phosphatidylcholine transfer protein (*PCTP*), S100 calcium-binding protein A12 (*S100A12*), S100 calcium-binding protein A8 (*S100A8*), and TNF receptor superfamily member 1B (*TNFRSF1B*)—were down-regulated.

3.2.2. Functional Enrichment Analysis and Protein–Protein Interactions

Gene Ontology functional enrichment for 28 DEGs was analyzed with DAVID. The data sorted by FDR value is included in Table 2. The top 5 of 46 biological processes included GO:0042632~cholesterol homeostasis; GO:0034375~high-density lipoprotein particle remodeling; GO:0043691~reverse cholesterol transport; GO:0010745~negative regulation of macrophage-derived foam cell differentiation; GO:0006869~lipid transport. The top 5 of 12 molecular functions included GO:0031210~phosphatidylcholine binding; GO:0001540~beta-amyloid binding; GO:0008289~lipid binding; GO:0034186~apolipoprotein A-I binding; GO:0071813~lipoprotein particle binding. The top 5 of 17 cellular components included GO:0005615~extracellular space, GO:0005576~extracellular region, GO:0034364~high-density lipoprotein particle, GO:0005886~plasma membrane, and GO:0009897~external side of plasma membrane (Table 2).

Table 2. Gene Ontology functional enrichment for DEGs in CAD relative to control. The FDR values are given.

| Term | Count | Genes | FDR |
|--|-------|--|------------------------|
| Biological Process | | | |
| GO:0042632~cholesterol homeostasis | 11 | ABCA1, SCARB1, CETP, ABCA5, NR1H2, LPL, LCAT, NR1H3, APOA1, APOE, LDLR | 5.03×10^{-14} |
| GO:0034375~high-density lipoprotein particle remodeling | 7 | SCARB1, CETP, ABCA5, LCAT, APOA1, APOE, PLTP | 8.94×10^{-12} |
| GO:0043691~reverse cholesterol transport | 7 | ABCA1, SCARB1, CETP, ABCA5, LCAT, APOA1, APOE | 1.38×10^{-11} |
| GO:0010745~negative regulation of macrophage derived foam cell differentiation | 6 | ABCA1, CETP, ABCA5, NR1H2, ITGB3, NR1H3 | 6.34×10^{-10} |
| GO:0006869~lipid transport | 8 | ABCA1, SCARB1, CETP, ABCA5, APOA1, PCTP, APOE, PLTP | 4.64×10^{-9} |
| GO:0010875~positive regulation of cholesterol efflux | 6 | ABCA1, NR1H2, NR1H3, APOA1, APOE, PLTP | 2.62×10^{-8} |
| GO:0034372~very-low-density lipoprotein particle remodeling | 5 | CETP, LPL, LCAT, APOA1, APOE | 2.99×10^{-8} |
| GO:0070328~triglyceride homeostasis | 6 | SCARB1, CETP, LPL, NR1H3, APOA1, APOE | 8.82×10^{-8} |
| GO:0008203~cholesterol metabolic process | 7 | ABCA1, CETP, ABCA5, LCAT, APOA1, APOE, LDLR | 8.82×10^{-8} |
| GO:0030301~cholesterol transport | 5 | CETP, ABCA5, LCAT, APOA1, LDLR | 1.20×10^{-6} |
| GO:0033344~cholesterol efflux | 5 | ABCA1, SCARB1, ABCA5, APOA1, APOE | 2.61×10^{-6} |
| GO:0006954~inflammatory response | 9 | IL1R1, IL1B, S100A12, TLR8, CD14, TNFRSF1B, CXCL5, S100A8, TNFRSF1A | 2.95×10^{-6} |

Table 2. Cont.

| Term | Count | Genes | FDR |
|---|-------|--|-----------------------|
| GO:0034384~high-density lipoprotein particle clearance | 4 | SCARB1, APOA1, APOE, LDLR | 3.62×10^{-6} |
| GO:0015914~phospholipid transport | 5 | SCARB1, CETP, PCTP, PLTP, LDLR | 9.50×10^{-6} |
| GO:0050729~positive regulation of inflammatory response | 6 | IL1B, LPL, S100A12, LDLR, S100A8, TNFRSF1A | 1.34×10^{-5} |
| GO:0034380~high-density lipoprotein particle assembly | 4 | ABCA1, APOA1, APOE, PRKACA | 1.84×10^{-5} |
| GO:0010867~positive regulation of triglyceride biosynthetic process | 4 | SCARB1, NR1H2, NR1H3, LDLR | 3.57×10^{-5} |
| GO:0006898~receptor-mediated endocytosis | 5 | AMN, ITGAM, CD14, APOE, LDLR | 1.23×10^{-4} |
| GO:0071222~cellular response to lipopolysaccharide | 6 | ABCA1, IL1B, NR1H3, CD14, TNFRSF1B, CXCL5 | 1.51×10^{-4} |
| GO:0006629~lipid metabolic process | 6 | NR1H2, LPL, LCAT, NR1H3, PLTP, LDLR | 2.98×10^{-4} |
| GO:0032369~negative regulation of lipid transport | 3 | NR1H2, ITGB3, NR1H3 | 2.98×10^{-4} |
| GO:0042158~lipoprotein biosynthetic process | 3 | LCAT, APOA1, APOE | 4.73×10^{-4} |
| GO:0032376~positive regulation of cholesterol transport | 3 | CETP, NR1H2, NR1H3 | 6.50×10^{-4} |
| GO:0070508~cholesterol import | 3 | SCARB1, APOA1, LDLR | 6.50×10^{-4} |
| GO:0032489~regulation of Cdc42 protein signal transduction | 3 | ABCA1, APOA1, APOE | 0.001163 |
| GO:0051006~positive regulation of lipoprotein lipase activity | 3 | NR1H2, NR1H3, APOA1 | 0.001794 |
| GO:0010887~negative regulation of cholesterol storage | 3 | ABCA1, NR1H2, NR1H3 | 0.002109 |
| GO:0033700~phospholipid efflux | 3 | ABCA1, APOA1, APOE | 0.00288 |
| GO:0071260~cellular response to mechanical stimulus | 4 | IL1B, ITGB3, TLR8, TNFRSF1A | 0.003053 |
| GO:0045723~positive regulation of fatty acid biosynthetic process | 3 | NR1H2, NR1H3, APOA1 | 0.003133 |
| GO:0032729~positive regulation of interferon-gamma production | 4 | IL1R1, IL1B, TLR8, CD14 | 0.003204 |
| GO:0030593~neutrophil chemotaxis | 4 | IL1B, S100A12, CXCL5, S100A8 | 0.003466 |
| GO:0055091~phospholipid homeostasis | 3 | ABCA1, CETP, APOA1 | 0.004246 |
| GO:0051044~positive regulation of membrane protein ectodomain proteolysis | 3 | IL1B, APOE, TNFRSF1B | 0.004632 |
| GO:0046470~phosphatidylcholine metabolic process | 3 | CETP, LCAT, APOA1 | 0.00616 |
| GO:0050728~negative regulation of inflammatory response | 4 | NR1H3, APOA1, APOE, TNFRSF1A | 0.012719 |
| GO:0006641~triglyceride metabolic process | 3 | CETP, LPL, APOE | 0.017257 |
| GO:0031663~lipopolysaccharide-mediated signaling pathway | 3 | SCARB1, IL1B, CD14 | 0.022846 |
| GO:0006644~phospholipid metabolic process | 3 | LPL, LCAT, APOA1 | 0.036972 |
| GO:0090108~positive regulation of high-density lipoprotein particle assembly | 2 | ABCA1, NR1H2 | 0.036972 |
| GO:0010899~regulation of phosphatidylcholine catabolic process | 2 | SCARB1, LDLR | 0.036972 |
| GO:0061771~response to caloric restriction | 2 | APOE, LDLR | 0.036972 |
| GO:0032757~positive regulation of interleukin-8 production | 3 | IL1B, TLR8, CD14 | 0.040866 |
| GO:0002790~peptide secretion | 2 | ABCA1, S100A8 | 0.043243 |
| GO:1902339~positive regulation of apoptotic process involved in morphogenesis | 2 | TNFRSF1B, TNFRSF1A | 0.043243 |

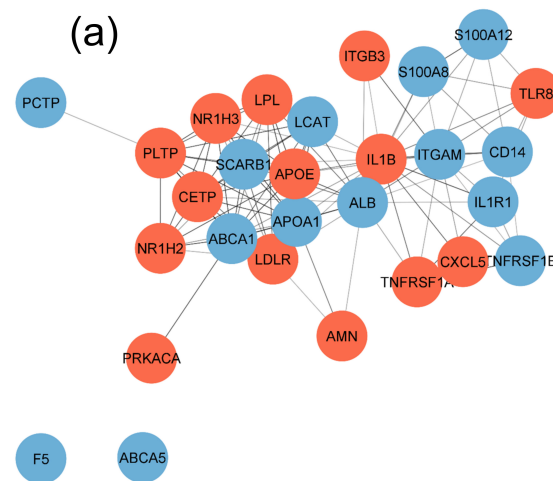
Table 2. Cont.

| Term | Count | Genes | FDR |
|---|-------|---|-----------------------|
| GO:0090107~regulation of high-density lipoprotein particle assembly | 2 | ABCA1, LCAT | 0.043243 |
| Molecular function | | | |
| GO:0031210~phosphatidylcholine binding | 5 | ABCA1, CETP, APOA1, PCTP, PLTP | 1.35×10^{-5} |
| GO:0001540~beta-amyloid binding | 5 | SCARB1, ITGAM, APOA1, APOE, LDLR | 3.40×10^{-4} |
| GO:0008289~lipid binding | 6 | SCARB1, CETP, APOA1, PCTP, APOE, PLTP | 3.40×10^{-4} |
| GO:0034186~apolipoprotein A-I binding | 3 | ABCA1, SCARB1, LCAT | 6.56×10^{-4} |
| GO:0071813~lipoprotein particle binding | 3 | LPL, APOE, LDLR | 0.001294 |
| GO:0015485~cholesterol binding | 4 | ABCA1, CETP, NR1H3, APOA1 | 0.001294 |
| GO:0008035~high-density lipoprotein particle binding | 3 | SCARB1, APOA1, PLTP | 0.002458 |
| GO:0030169~low-density lipoprotein particle binding | 3 | SCARB1, PLTP, LDLR | 0.004408 |
| GO:0034185~apolipoprotein binding | 3 | ABCA1, SCARB1, LPL | 0.004408 |
| GO:0005319~lipid transporter activity | 3 | ABCA1, ABCA5, APOE | 0.011161 |
| GO:0005102~receptor binding | 5 | ABCA1, AMN, LPL, APOA1, APOE | 0.030793 |
| GO:0005507~copper ion binding | 3 | ALB, S100A12, F5 | 0.035664 |
| Cellular component | | | |
| GO:0005615~extracellular space | 16 | CETP, AMN, ITGAM, APOA1, LPL, LCAT, CXCL5, F5, TNFRSF1A, IL1B, ALB, S100A12, CD14, APOE, PLTP, S100A8 | 2.71×10^{-7} |
| GO:0005576~extracellular region | 16 | CETP, IL1R1, APOA1, LPL, LCAT, TNFRSF1B, CXCL5, F5, TNFRSF1A, IL1B, ALB, S100A12, CD14, APOE, PLTP, S100A8 | 4.41×10^{-7} |
| GO:0034364~high-density lipoprotein particle | 5 | CETP, LCAT, APOA1, APOE, PLTP | 1.55×10^{-6} |
| GO:0005886~plasma membrane | 19 | ABCA1, SCARB1, AMN, ITGAM, ABCA5, IL1R1, ITGB3, APOA1, LPL, TNFRSF1B, F5, TNFRSF1A, S100A12, TLR8, CD14, APOE, PRKACA, LDLR, S100A8 | 2.95×10^{-4} |
| GO:0009897~external side of plasma membrane | 7 | ABCA1, ITGAM, IL1R1, ITGB3, TLR8, CD14, LDLR | 6.99×10^{-4} |
| GO:0070062~extracellular exosome | 12 | SCARB1, CETP, AMN, ITGAM, ITGB3, ALB, LCAT, APOA1, CD14, APOE, PRKACA, S100A8 | 0.001074 |
| GO:0042627~chylomicron | 3 | LPL, APOA1, APOE | 0.002452 |
| GO:0043235~receptor complex | 5 | AMN, ITGB3, NR1H3, LDLR, TNFRSF1A | 0.002594 |
| GO:0034361~very-low-density lipoprotein particle | 3 | LPL, APOA1, APOE | 0.004377 |
| GO:0009986~cell surface | 6 | SCARB1, ITGAM, ITGB3, LPL, LDLR, TNFRSF1A | 0.014727 |
| GO:0005794~Golgi apparatus | 7 | ABCA1, ABCA5, ALB, CD14, APOE, LDLR, F5 | 0.031004 |
| GO:0030139~endocytic vesicle | 3 | ABCA1, AMN, APOA1 | 0.033311 |
| GO:0045121~membrane raft | 4 | ABCA1, CD14, TNFRSF1B, TNFRSF1A | 0.033311 |

Table 2. *Cont.*

| Term | Count | Genes | FDR |
|---|-------|---------------------------|----------|
| GO:0010008~endosome membrane | 4 | AMN, TLR8, CD14, LDLR | 0.037424 |
| GO:0002947~tumor necrosis factor receptor superfamily complex | 2 | TNFRSF1B, TNFRSF1A | 0.032813 |
| GO:0005788~endoplasmic reticulum lumen | 4 | ALB, APOA1, APOE, F5 | 0.041851 |
| GO:0005764~lysosome | 4 | SCARB1, ABCA5, IL1B, LDLR | 0.041851 |

The PPI network created with STRING and exported to Cytoscape is given in Figure 2a for protein products of 28 DEGs. Thirteen of the forty significant KEGG pathways sorted by FDR and gene count (equal or higher than 4) are included in Figure 2b. They included cholesterol metabolism, Hematopoietic cell lineage, Amoebiasis, PPAR signaling pathway, Pertussis, Human cytomegalovirus infection, NF-kappa B signaling pathway, TNF signaling pathway, Osteoclast differentiation, Fluid shear stress and atherosclerosis, MAPK signaling pathway, Cytokine–cytokine receptor interaction, and Phagosome. Furthermore, the Toll-like receptor signaling pathway and the IL-17 signaling pathway, each with three participating nodes, were detected as well. Thus, both lipid, inflammation, and innate immunity-associated pathways are significant in CAD.



(b)

| KEGG Pathway | Gene Count | Matching Proteins | FDR |
|---|------------|---|------------------------|
| hsa04979: Cholesterol metabolism | 9 | CETP, APOA1, APOE, SCARB1, LCAT, LPL, ABCA1, PLTP, LDLR | 1.71×10^{-14} |
| hsa04640: Hematopoietic cell lineage | 5 | IL1B, CD14, IL1R1, ITGAM, ITGB3 | 3.84×10^{-5} |
| hsa05146: Amoebiasis | 5 | IL1B, CD14, PRKACA, IL1R1, ITGAM | 4.01×10^{-5} |
| hsa03320: PPAR signaling pathway | 4 | APOA1, LPL, PLTP, NR1H3 | 3.70×10^{-4} |
| hsa05133: Pertussis | 4 | IL1B, CXCL5, CD14, ITGAM | 3.70×10^{-4} |
| hsa05163: Human cytomegalovirus infection | 5 | TNFRSF1A, IL1B, PRKACA, IL1R1, ITGB3 | 8.10×10^{-4} |
| hsa04064: NF-kappa B signaling pathway | 4 | TNFRSF1A, IL1B, CD14, IL1R1 | 8.10×10^{-4} |
| hsa04668: TNF signaling pathway | 4 | TNFRSF1A, IL1B, CXCL5, TNFRSF1B | 9.00×10^{-4} |
| hsa04380: Osteoclast differentiation | 4 | TNFRSF1A, IL1B, IL1R1, ITGB3 | 0.0011 |

Figure 2. *Cont.*

| | | | |
|--|---|--|--------|
| hsa05418: Fluid shear stress and atherosclerosis | 4 | TNFRSF1A, IL1B, IL1R1, ITGB3 | 0.0012 |
| hsa04010: MAPK signaling pathway | 5 | TNFRSF1A, IL1B, CD14, PRKACA, IL1R1 | 0.0014 |
| hsa04060: Cytokine-cytokine receptor interaction | 5 | TNFRSF1A, IL1B, CXCL5, TNFRSF1B, IL1R1 | 0.0014 |
| hsa04145: Phagosome | 4 | SCARB1, CD14, ITGAM, ITGB3 | 0.0014 |

Figure 2. Interaction of proteins coded by differentially expressed genes in CAD patients. (a) the full STRING network was created with Cytoscape. The number of nodes is 28, number of edges is 110, and PPI enrichment is lower 1.0×10^{-16} . Upregulated and downregulated genes are marked by red and blue colors, respectively. (b) Top 13 KEGG pathways were sorted by gene number (4–9) and FDR values lower than 0.0015.

3.3. Association of Transcripts with Lipids in Control and CAD Cohorts

3.3.1. Bivariate Correlations between Transcript and Lipid Levels

The associations between lipid and apolipoprotein content and gene expression were studied by correlation analysis for two patient cohorts separately. The significant correlations for the HDL cluster given as Pearson coefficients are included in Table 3.

Table 3. Correlations between expression of genes within the HDL cluster and plasma lipoprotein and apoA-I levels in control and CAD cohorts. Pearson correlation coefficients r and p -values in brackets are given only for significant correlations ($p < 0.05$) and controlled with the Benjamini–Hochberg procedure with FDR values of 0.20 (control) and 0.05 (CAD cohort).

| Gene | HDL-C | TG | Chol | apoA-I |
|---------------|----------------|----------------|----------------|----------------|
| Control | | | | |
| <i>APOA1</i> | | | 0.323 (0.011) | |
| <i>CUBN</i> | −0.322 (0.010) | | −0.305 (0.015) | |
| <i>HDLBP</i> | | | −0.324 (0.010) | |
| <i>LCAT</i> | | | | −0.336 (0.008) |
| <i>SOAT1</i> | −0.397 (0.002) | | | |
| CAD | | | | |
| <i>ABCG1</i> | 0.294 (0.010) | | | 0.273 (0.018) |
| <i>ALB</i> | 0.451 (0.000) | | 0.343 (0.002) | 0.453 (0.000) |
| <i>AMN</i> | | | | 0.304 (0.008) |
| <i>BMP1</i> | −0.332 (0.003) | | | −0.345 (0.002) |
| <i>CUBN</i> | 0.546 (0.000) | −0.375 (0.001) | | 0.553 (0.000) |
| <i>HDLBP</i> | 0.335 (0.003) | | | 0.371 (0.001) |
| <i>HMGCR</i> | −0.314 (0.006) | | | −0.319 (0.005) |
| <i>LCAT</i> | −0.319 (0.005) | | −0.330 (0.004) | −0.426 (0.000) |
| <i>PLTP</i> | | | | −0.287 (0.012) |
| <i>PRKACB</i> | −0.438 (0.000) | 0.366 (0.001) | | −0.475 (0.000) |
| <i>PRKACG</i> | 0.414 (0.000) | −0.345 (0.002) | | 0.394 (0.001) |
| <i>SOAT1</i> | −0.353 (0.002) | | | −0.388 (0.001) |

For the control cohort, HDL-C was negatively associated with cubilin (*CUBN*) and sterol O-acyltransferase 1 (*SOAT1*) transcripts. Total cholesterol was positively associated with *APOA1*, while it was negatively associated with *CUBN* and high-density lipoprotein binding protein (*HDLBP*). ApoA-I was negatively associated with the lecithin-cholesterol acyltransferase (*LCAT*) transcript.

For CAD patients, HDL-C was positively associated with the transcripts of genes coding cholesterol transporter ATP binding cassette subfamily G member 1 (*ABCG1*), albumin (*ALB*), and other proteins involved in cholesterol metabolism (*CUBN*, *HDLBP*, and protein kinase cAMP-activated catalytic subunit gamma (*PRKACG*)). However, HDL-C was negatively associated with bone morphogenetic protein 1 (*BMP1*), *LCAT*, *SOAT1*, and protein kinase cAMP-activated catalytic subunit beta (*PRKACB*) transcripts. Importantly, HDL-C was negatively associated with the 3-hydroxy-3-methylglutaryl-CoA reductase

(*HMGCR*) transcript. The associations between apoA-I and transcript levels generally included the above-mentioned associations for HDL-C with the addition of a positive association between apoA-I and amnion-associated transmembrane protein (*AMN*) transcript and a negative association between apoA-I and phospholipid transfer protein (*PLTP*). Plasma TG were associated with transcripts generally in a manner reciprocal to HDL-C.

The significant associations for the transcripts of atherogenesis-prone genes are included in Table 4. In the control cohort, HDL-C was negatively associated with microsomal glutathione S-transferase 1 (*MGST1*) and *TLR8* transcripts. Total cholesterol and TG were not associated with any transcript in the atherogen cluster.

Table 4. Correlations between expression of genes within the atherogen cluster and plasma lipoprotein and apoA-I levels in control and CAD cohorts. Pearson correlation coefficients (r and p values in brackets) are given only for significant correlations ($p < 0.05$) and controlled with the Benjamini–Hochberg procedure with an FDR value of 0.05.

| Gene | HDL-C | TG | Chol | apoA-I |
|----------------|----------------|---------------|----------------|----------------|
| Control | | | | |
| <i>MGST1</i> | −0.393 (0.002) | | | −0.434 (0.001) |
| <i>TLR8</i> | −0.378 (0.002) | | | |
| CAD | | | | |
| <i>CD14</i> | −0.430 (0.000) | | | −0.426 (0.000) |
| <i>CD36</i> | −0.570 (0.000) | 0.335 (0.003) | −0.441 (0.000) | −0.571 (0.000) |
| <i>CYBA</i> | −0.334 (0.003) | | | −0.363 (0.001) |
| <i>F5</i> | −0.357 (0.002) | | | −0.364 (0.001) |
| <i>MGST1</i> | −0.270 (0.018) | | | −0.333 (0.003) |
| <i>NPC2</i> | −0.357 (0.002) | | −0.366 (0.001) | −0.370 (0.001) |
| <i>OLR1</i> | −0.367 (0.001) | 0.416 (0.000) | | −0.346 (0.002) |
| <i>PRKCQ</i> | 0.455 (0.000) | | | 0.429 (0.000) |
| <i>S100A12</i> | −0.438 (0.000) | | | −0.443 (0.000) |
| <i>S100A8</i> | −0.452 (0.000) | | | −0.413 (0.000) |
| <i>S100A9</i> | −0.406 (0.000) | | | −0.364 (0.001) |
| <i>SLPI</i> | −0.381 (0.001) | 0.430 (0.000) | | −0.396 (0.000) |
| <i>SREBF1</i> | 0.316 (0.005) | | | |
| <i>TLR5</i> | −0.322 (0.005) | | | −0.354 (0.002) |
| <i>TLR8</i> | −0.349 (0.002) | | | −0.337 (0.003) |
| <i>VEGFA</i> | −0.346 (0.002) | | | −0.232 (0.004) |

For CAD patients, HDL-C was positively associated with the transcripts of two genes: protein kinase C theta (*PRKCQ*) and sterol regulatory element binding transcription factor 1 (*SREBF1*). HDL-C and apoA-I were negatively associated with the following fourteen transcripts: CD14 molecule (*CD14*), CD36 molecule (*CD36*), cytochrome b-245 alpha chain (*CYBA*), coagulation factor V (*F5*), *MGST1*, NPC intracellular cholesterol transporter 2 (*NPC2*), oxidized low-density lipoprotein receptor 1 (*OLR1*), S100 calcium-binding protein A12 (*S100A12*), S100 calcium-binding protein A8 (*S100A8*), S100 calcium-binding protein A9 (*S100A9*), secretory leukocyte peptidase inhibitor (*SLPI*), Toll-like receptor 5 (*TLR5*), Toll-like receptor 8 (*TLR8*), and vascular endothelial growth factor A (*VEGFA*). Plasma TG was associated with transcripts generally in a manner reciprocal to HDL-C. Notably, total cholesterol was negatively associated with *CD36* and *NPC2* transcripts, analogously to HDL-C.

3.3.2. Contribution of Transcript to HDL-C Level by Multiple Regression

To estimate the contribution of gene transcripts to HDL-C levels, multiple linear regression was used for two cohorts separately. To increase statistical power, only transcripts significantly correlated with HDL-C and passed through the control for multiple comparisons, plasma TG, non-HDL-C, and age were included in the analysis as independent variables. Multiple regression data are included in Table 5. For the control cohort, HDL-C

was positively associated with non-HDL-C while negatively associated with *TLR8*, *SOAT1*, and plasma TG. Four independent predictors with VIF values close to 1 controlled up to 59% of HDL-C variability. For CAD patients, HDL-C was positively associated with *PRKACG*, *PRKCQ*, *SREBF1*, and nonHDL-C, while negatively associated with *PRKACB*, *LCAT*, *S100A8*, and plasma TG. Eight independent predictors with VIF values 1.18–1.68 controlled up to 79% of HDL-C variability.

Table 5. The contribution of plasma lipid and transcripts of genes from HDL-cluster and atherogen cluster to HDL-C levels in control and CAD cohorts. Transcripts significantly correlated with HDL-C by pairwise comparison were included, together with age, TG, and non-HDL-C as independent variables. Forward and backward stepwise multiple linear regression analysis was performed until the coincidence of both equations. R^2 value equals explained variability. The variance inflation factor (VIF) is a measure of multicollinearity (values lower than 4 correspond to negligible multicollinearity). The Darbin–Watson statistic DW serves as a *test* for checking autocorrelation in the residuals (no first-order autocorrelation is assumed for DW values 1.50–2.50).

| | Independent Variable | $\beta \pm \text{SEM}$ | p | R^2 | VIF | DW |
|----------------------|----------------------|------------------------|-------|-------|------|------|
| Control ($n = 54$) | | | | 0.594 | | 1.76 |
| | <i>SOAT1</i> | -0.521 ± 0.094 | 0.000 | | 1.08 | |
| | <i>TLR8</i> | -0.222 ± 0.095 | 0.023 | | 1.08 | |
| | nonHDL-C | 0.265 ± 0.098 | 0.009 | | 1.16 | |
| | TG | -0.319 ± 0.098 | 0.002 | | 1.16 | |
| CAD ($n = 75$) | | | | 0.785 | | 1.70 |
| | <i>PRKACB</i> | -0.273 ± 0.064 | 0.000 | | 1.27 | |
| | <i>PRKACG</i> | 0.190 ± 0.062 | 0.003 | | 1.18 | |
| | <i>LCAT</i> | -0.340 ± 0.071 | 0.000 | | 1.53 | |
| | <i>PRKCQ</i> | 0.166 ± 0.074 | 0.028 | | 1.68 | |
| | <i>S100A8</i> | -0.216 ± 0.072 | 0.004 | | 1.60 | |
| | <i>SREBF1</i> | 0.306 ± 0.071 | 0.000 | | 1.54 | |
| | nonHDL-C | 0.206 ± 0.071 | 0.005 | | 1.56 | |
| | TG | -0.243 ± 0.074 | 0.002 | | 1.70 | |

4. Discussion

Numerous studies have sought to identify gene expression signatures of CAD risk by measuring mRNA in peripheral blood, but only a few candidate transcripts have been validated across studies [43]. The use of two gene sets related to HDL metabolism and atherogenesis predefined by us earlier by the system biology approach [31] permitted us to reach a 43% hit rate (28 from 65 genes) to reveal gene expression changes at CAD. Notably, two gene clusters were selected ab initio, thus eliminating the labor-consuming transcriptomics sequencing analysis in experimental studies [44,45] or the initial search for gene significance in in silico approaches [46,47].

The major novelties of our study are, firstly, the use of peripheral blood mononuclear cells (PBMC) from CAD patients unaffected by lipid-lowering therapy known to profoundly change lipoprotein metabolism; secondly, the down-regulation of the expression of genes involved in cholesterol efflux and reverse cholesterol transport in CAD; thirdly, the involvement of six signaling pathways connected to inflammation and innate immunity in CAD; and, finally, the different contribution of transcript level to HDL-C concentration for CAD and control patients. A gender-specific approach was applied in our study due to a higher CAD mortality rate in men compared to women, a different clinical picture of coronary heart disease, and distinctive risk factors in women [48]. Thus, the associations of HDL-C level with the expression of genes involved in HDL metabolism and atherogenesis for a future targeted personalized therapy are primarily limited to only middle-aged male patients with CAD. The other limitation of the study is the absence of data on the level of protein products of the genes studied. However, a close coincidence of mRNA expression

and protein levels is known [42], at least for several genes described in the present study. The direct relationship between transcript level and protein activity is assumed hereinafter.

Three aspects are important in the analysis of differential gene expression at CAD and the contribution of transcripts to HDL-C level: (1) RCT and cholesterol efflux; (2) cholesterol synthesis and uptake; (3) intracellular cholesterol trafficking [49]. The data on the expression profile and contribution of transcript level to HDL-C concentration are discussed successively.

By differential expression, the expression of *NR1H2* and *NR1H3* LXR-receptors was up-regulated in CAD patients compared to controls, which may be related to the accumulation of intracellular cholesterol in coronary artery disease. Moreover, the expression of *ABCA1*, *ABCA5*, *SCARB1*, *ALB*, *APOA1*, and *LCAT*, all belonging to the major participants in reverse cholesterol transport, was down-regulated, evidencing RCT deficiency at CAD. Notably, *LDLR* and *APOE* were up-regulated; apoE may compensate for apoA-I deficiency in the cholesterol efflux reaction [50]. The increased expression of *LDLR* in CAD patients compared to controls seems to underlie the decrease of LDL-C in the plasma of CAD patients due to the increased clearance of LDL through the hepatic LDL receptor [51]. Based on the decreased cholesterol content in a single LDL particle, an increased percentage of cholesterol-depleted small dense LDL (sdLDL) in CAD patients is suggested. These particles demonstrate prolonged circulation time, likely due to a lower affinity for the LDL receptor [52]. The increased expression of *LPL* at CAD, which stimulates selective uptake of cholesteryl esters from LDL via pathways that are distinct from SR-BI [53], seems to also contribute to the generation of sdLDL. Furthermore, the LPL present in the arterial wall may, by binding to LDL, increase the residence time of LDL in the arterial wall, thus promoting atherogenesis [54]. However, the change in intracellular cholesterol levels is not definitely evident. A simplest sequential kinetic scheme of reverse cholesterol transport may include (i) cholesterol efflux to lipid-free apoA-I by ABCA1 in macrophages; (ii) cholesteryl ester formation in nascent pre β -HDL and mature α -HDL catalyzed by LCAT; (iii) selective removal of cholesteryl ester from α -HDL by SR-BI in hepatocytes with the generation of CE-depleted HDL*: apoA-I (via ABCA1) \rightarrow pre β -HDL (via LCAT) \rightarrow α -HDL \rightarrow HDL* (via SR-BI). Within this scheme, cholesterol efflux is a first and rate-limiting step, and a residual RCT efficiency of 73–79% in CAD compared to control may be reasonably assumed based on *APOA1* and *ABCA1* expression changes (Figure 1).

The systemic inflammation in CAD patients is evidenced by several findings. First, the proinflammatory *IL1B* is up-regulated. Antagonism of interleukin-1 β reduces coronary heart disease in patients with a previous myocardial infarction and evidence of systemic inflammation. IL-1 β and IL-18 are produced via the NLRP3 inflammasome in myeloid cells in response to cholesterol accumulation [28], thus supporting our suggestion on the accumulation of intracellular cholesterol in PBMC from CAD patients. The up-regulation of *IL1B* and *TNFRSF1A* genes contributes to the NF-kappa B signaling pathway. Second, the increased expression of *TLR5* and *TLR8* as dominant components of the innate immune system [55] contributes to the Toll-like receptor signaling pathway. Third, *CXCL5* chemokine expression was up-regulated. *CXCL5* has pro-inflammatory effects, mainly through the recruitment of monocytes by the CXCR2 receptor [56].

The above-mentioned proinflammatory shift in gene expression at CAD may be counterbalanced by down-regulation of *IL1R1*, *CD14*, *TNFRSF1B*, *S100A8*, and *ITGAM* genes. First, *IL1R1*/IL1 β augment both megakaryocyte and platelet functions, thereby promoting a prothrombotic environment and potentially contributing to the development of atherothrombotic disease [57]. Second, *CD14* is suggested to underlie the contribution of intermediate CD14⁺⁺CD16⁺ monocyte counts that predict cardiovascular events [58]. Third, *TNFRSF1B* has been related to cardiovascular disease and mortality in the Framingham Heart Study [59]. Fourth, *S100A8* has mainly been implicated in cardiovascular disease [60]. Finally, *ITGAM* has been identified as an inducer of coronary atherosclerosis through endothelial cell dysfunction [61]. Moreover, the expression of the adhesion receptor integrin *ITGB3* was up-regulated at CAD in the present study. The *ITGB3* molecule is consistently

detected on macrophages in early and advanced human atherosclerotic lesions, and its expression is up-regulated by atherogenic stimuli [62]. Furthermore, macrophage beta3 integrin, acting through TNFalpha, suppressed inflammation caused by hyperlipidemia attributable to high-fat feeding [63].

For the control cohort, the significance of transcript level as independent predictor of HDL-C variability by multiple regression revealed the negative contributions of *TLR8* and *SOAT1* expression to HDL-C variability. *TLR8*, as a negative predictor of HDL-C level and a dominant component of the innate immune system [55], assumes HDL's atheroprotective property. *SOAT1* as a negative predictor of HDL-C level may be associated with the increase in intracellular free cholesterol pool available for efflux at hyperalphalipoproteinemia in controls. The negative contribution of plasma TG to HDL-C level may originate first from the generation of nascent HDL [64] at TG lipolysis in TG-rich lipoproteins and, second, from the increased hetero-exchange of cholesteryl ester and triglyceride molecules between HDL and VLDL particles at the increase of plasma TG with the subsequent hydrolysis of TG in HDL [3].

For the CAD cohort, eight independent predictors of HDL-C variability were revealed by multiple regression. A positive contribution of *SREBF1* expression up-regulated by liver X receptors assures a supply of fatty acids during sterol overloading at hyperalphalipoproteinemia to allow storage of excess cholesterol as cholesteryl ester [16]. The *LCAT* transcript as a negative predictor of HDL-C level assumes RCT impairment at CAD. *PRKACG* is a central actor in platelet biogenesis [65] and also a positive predictor of HDL-C level. The latter may be associated with the increase in platelet activation with the increase in HDL-C at CAD. The loss of the *PRKAC*β2 splice variant, the latter being measured in our study, can increase the inflammatory susceptibility of macrophages [66] and Cβ2 transcripts were reduced in human fibroatheroma, which may cause plaque progression [67]. Thus, HDL's proatherogenic property follows from the negative contribution of *PRKACB* to HDL-C variability. Also, the proatherogenic property of HDL deduced from the positive contribution of *PRKCQ* to HDL-C variability follows from the involvement of protein kinase C theta in thrombin-induced CD36 expression and foam cell formation; the inhibition of protein kinase C theta decreases atherosclerotic lesions and improves insulin sensitivity [68]. *S100A8* has mainly been implicated in cardiovascular disease by promoting vascular endothelial cell dysfunction and apoptosis [60]. The negative contribution of *S100A8* to HDL-C levels thereby assumes HDL's atheroprotective property in CAD patients. Overall, both atheroprotective (via *S100A8* expression) and proatherogenic (via *SREBF1*, *LCAT*, *PRKACG*, *PRKACB*, and *PRKCQ* expression) properties of HDL seem to exist in CAD patients. However, the causal relationships between HDL-C and transcript levels remain to be elucidated.

5. Conclusions

For control patients, the negative contributions of *TLR8* and *SOAT1* transcripts to HDL-C levels assume "full" HDL functionality. However, for CAD patients, the efficiency of reverse cholesterol transport is 73–79%, and intracellular cholesterol accumulates with the increase of HDL-C. More functional and compositional studies are needed to evaluate the "residual" HDL functionality. The measurements of the cholesterol efflux capacity of HDL preparations are now in progress. Also, the future estimations of the expression profiles for low, normal, and elevated HDL-C concentrations in CAD seem to clarify the existing uncertainty about the exact nature of HDL functionality. Systemic inflammation in CAD patients may be limited by up-regulation of *APOE* and *ITGB3* and down-regulation of *IL1R1*, *CD14*, *TNFRSF1B*, *S100A8*, and *ITGAM*. Both the selected key genes and signal pathways, derived from analysis of protein–protein interactions, may represent HDL-specific targets for diagnosis and treatment of atherogenesis.

Supplementary Materials: The following supporting information can be downloaded at: <https://www.mdpi.com/article/10.3390/cimb45080431/s1>, Supplementary Table S1: The primers used in RT-PCR.

Author Contributions: Conceptualization, A.D.D.; Writing—Draft Preparation, A.D.D. and E.V.N.; Investigation, E.V.N., A.V.R., V.B.B. and M.A.V.; Figure and Tables, A.V.R. and V.B.B., Writing—Review and Editing, A.D.D., E.V.N. and L.V.D.; Patients, M.A.P.; Supervision, A.D.D. and L.V.D.; Curation and Project Administration, L.V.D. and S.A.L. All authors have read and agreed to the published version of the manuscript.

Funding: This research received no external funding.

Institutional Review Board Statement: The study protocol conforms to the ethical guidelines of the 1975 Declaration of Helsinki and has been approved by the local ethics committee on research on humans.

Informed Consent Statement: Written informed consent was obtained from each patient included in the study.

Data Availability Statement: The data presented in this study are available on request from the corresponding author.

Conflicts of Interest: The authors declare no conflict of interest.

References

1. Groenen, A.G.; Halmos, B.; Tall, A.R.; Westerterp, M. Cholesterol efflux pathways, inflammation, and atherosclerosis. *Crit. Rev. Biochem. Mol. Biol.* **2021**, *56*, 426–439. [[CrossRef](#)]
2. Rasheed, A.; Cummins, C.L. Beyond the Foam Cell: The Role of LXRs in Preventing Atherogenesis. *Int. J. Mol. Sci.* **2018**, *19*, 2307. [[CrossRef](#)]
3. Dergunov, A.D.; Baserova, V.B. Different Pathways of Cellular Cholesterol Efflux. *Cell Biochem. Biophys.* **2022**, *80*, 471–481. [[CrossRef](#)] [[PubMed](#)]
4. Khera, A.V.; Cuchel, M.; Llera-Moya, M.; Rodrigues, A.; Burke, M.F.; Jafri, K.; French, B.C.; Phillips, J.A.; Mucksavage, M.L.; Wilensky, R.L.; et al. Cholesterol efflux capacity, high-density lipoprotein function, and atherosclerosis. *N. Engl. J. Med.* **2011**, *364*, 127–135. [[CrossRef](#)] [[PubMed](#)]
5. Abe, R.J.; Abe, J.I.; Nguyen, M.T.H.; Olmsted-Davis, E.A.; Mamun, A.; Banerjee, P.; Cooke, J.P.; Fang, L.; Pownall, H.; Le, N.T. Free Cholesterol Bioavailability and Atherosclerosis. *Curr. Atheroscler. Rep.* **2022**, *24*, 323–336. [[CrossRef](#)] [[PubMed](#)]
6. Agarwala, A.P.; Rodrigues, A.; Risman, M.; McCoy, M.; Trindade, K.; Qu, L.; Cuchel, M.; Billheimer, J.; Rader, D.J. High-Density Lipoprotein (HDL) Phospholipid Content and Cholesterol Efflux Capacity Are Reduced in Patients With Very High HDL Cholesterol and Coronary Disease. *Arterioscler. Thromb. Vasc. Biol.* **2015**, *35*, 1515–1519. [[CrossRef](#)]
7. Josefs, T.; Wouters, K.; Tietge, U.J.F.; Annema, W.; Dullaart, R.P.F.; Vaisar, T.; Arts, I.C.W.; van der Kallen, C.J.H.; Stehouwer, C.D.A.; Schalkwijk, C.G.; et al. High-density lipoprotein cholesterol efflux capacity is not associated with atherosclerosis and prevalence of cardiovascular outcome: The CODAM study. *J. Clin. Lipidol.* **2020**, *14*, 122–132. [[CrossRef](#)]
8. Asztalos, B.F.; Llera-Moya, M.; Dallal, G.E.; Horvath, K.V.; Schaefer, E.J.; Rothblat, G.H. Differential effects of HDL subpopulations on cellular ABCA1- and SR-BI-mediated cholesterol efflux. *J. Lipid Res.* **2005**, *46*, 2246–2253. [[CrossRef](#)]
9. Chen, L.; Zhao, Z.W.; Zeng, P.H.; Zhou, Y.J.; Yin, W.J. Molecular mechanisms for ABCA1-mediated cholesterol efflux. *Cell Cycle* **2022**, *21*, 1121–1139. [[CrossRef](#)]
10. Matsuo, M. ABCA1 and ABCG1 as potential therapeutic targets for the prevention of atherosclerosis. *J. Pharmacol. Sci.* **2022**, *148*, 197–203. [[CrossRef](#)]
11. Camont, L.; Chapman, M.J.; Kontush, A. Biological activities of HDL subpopulations and their relevance to cardiovascular disease. *Trends Mol. Med.* **2011**, *17*, 594–603. [[CrossRef](#)] [[PubMed](#)]
12. Shen, W.J.; Azhar, S.; Kraemer, F.B. SR-B1: A Unique Multifunctional Receptor for Cholesterol Influx and Efflux. *Annu. Rev. Physiol.* **2018**, *80*, 95–116. [[CrossRef](#)]
13. Han, J.; Nicholson, A.C.; Zhou, X.; Feng, J.; Gotto, A.M., Jr.; Hajjar, D.P. Oxidized low density lipoprotein decreases macrophage expression of scavenger receptor B-I. *J. Biol. Chem.* **2001**, *276*, 16567–16572. [[CrossRef](#)] [[PubMed](#)]
14. Ji, A.; Wroblewski, J.M.; Webb, N.R.; van der Westhuyzen, D.R. Impact of phospholipid transfer protein on nascent high-density lipoprotein formation and remodeling. *Arterioscler. Thromb. Vasc. Biol.* **2014**, *34*, 1910–1916. [[CrossRef](#)] [[PubMed](#)]
15. Horton, J.D.; Goldstein, J.L.; Brown, M.S. SREBPs: Activators of the complete program of cholesterol and fatty acid synthesis in the liver. *J. Clin. Investig.* **2002**, *109*, 1125–1131. [[CrossRef](#)]
16. Repa, J.J.; Liang, G.; Ou, J.; Bashmakov, Y.; Lobaccaro, J.M.; Shimomura, I.; Shan, B.; Brown, M.S.; Goldstein, J.L.; Mangelsdorf, D.J. Regulation of mouse sterol regulatory element-binding protein-1c gene (SREBP-1c) by oxysterol receptors, LXRalpha and LXRbeta. *Genes Dev.* **2000**, *14*, 2819–2830. [[CrossRef](#)]

17. Russo-Savage, L.; Schulman, I.G. Liver X receptors and liver physiology. *Biochim. Biophys. Acta Mol. Basis Dis.* **2021**, *1867*, 166121. [[CrossRef](#)]
18. Cheng, Y.; Manabe, I.; Hayakawa, S.; Endo, Y.; Oishi, Y. Caspase-11 contributes to site-1 protease cleavage and SREBP1 activation in the inflammatory response of macrophages. *Front. Immunol.* **2023**, *14*, 1009973. [[CrossRef](#)]
19. Im, S.S.; Yousef, L.; Blaschitz, C.; Liu, J.Z.; Edwards, R.A.; Young, S.G.; Raffatellu, M.; Osborne, T.F. Linking lipid metabolism to the innate immune response in macrophages through sterol regulatory element binding protein-1a. *Cell Metab.* **2011**, *13*, 540–549. [[CrossRef](#)]
20. Peng, C.; Lei, P.; Li, X.; Xie, H.; Yang, X.; Zhang, T.; Cao, Z.; Zhang, J. Down-regulated of SREBP-1 in circulating leukocyte is a risk factor for atherosclerosis: A case control study. *Lipids Health Dis.* **2019**, *18*, 177. [[CrossRef](#)]
21. Perez-Belmonte, L.M.; Moreno-Santos, I.; Cabrera-Bueno, F.; Sanchez-Espin, G.; Castellano, D.; Such, M.; Crespo-Leiro, M.G.; Carrasco-Chinchilla, F.; Alonso-Pulpon, L.; Lopez-Garrido, M.; et al. Expression of Sterol Regulatory Element-Binding Proteins in epicardial adipose tissue in patients with coronary artery disease and diabetes mellitus: Preliminary study. *Int. J. Med.Sci.* **2017**, *14*, 268–274. [[CrossRef](#)]
22. Goldstein, J.L.; DeBose-Boyd, R.A.; Brown, M.S. Protein sensors for membrane sterols. *Cell* **2006**, *124*, 35–46. [[CrossRef](#)] [[PubMed](#)]
23. Yu, X.H.; Fu, Y.C.; Zhang, D.W.; Yin, K.; Tang, C.K. Foam cells in atherosclerosis. *Clin. Chim. Acta* **2013**, *424*, 245–252. [[CrossRef](#)] [[PubMed](#)]
24. Heisler, D.B.; Johnson, K.A.; Ma, D.H.; Ohlson, M.B.; Zhang, L.; Tran, M.; Corley, C.D.; Abrams, M.E.; McDonald, J.G.; Schoggins, J.W.; et al. A concerted mechanism involving ACAT and SREBPs by which oxysterols deplete accessible cholesterol to restrict microbial infection. *Elife* **2023**, *12*, e83534. [[CrossRef](#)]
25. Li, Q.; Wang, M.; Zhang, S.; Jin, M.; Chen, R.; Luo, Y.; Sun, X. Single-cell RNA sequencing in atherosclerosis: Mechanism and precision medicine. *Front. Pharmacol.* **2022**, *13*, 977490. [[CrossRef](#)]
26. Cochain, C.; Vafadarnejad, E.; Arampatzi, P.; Pelisek, J.; Winkels, H.; Ley, K.; Wolf, D.; Saliba, A.E.; Zerneck, A. Single-Cell RNA-Seq Reveals the Transcriptional Landscape and Heterogeneity of Aortic Macrophages in Murine Atherosclerosis. *Circ. Res.* **2018**, *122*, 1661–1674. [[CrossRef](#)]
27. Kim, K.; Shim, D.; Lee, J.S.; Zaitsev, K.; Williams, J.W.; Kim, K.W.; Jang, M.Y.; Seok, J.H.; Yun, T.J.; Lee, S.H.; et al. Transcriptome Analysis Reveals Nonfoamy Rather Than Foamy Plaque Macrophages Are Proinflammatory in Atherosclerotic Murine Models. *Circ. Res.* **2018**, *123*, 1127–1142. [[CrossRef](#)]
28. Westerterp, M.; Fotakis, P.; Ouimet, M.; Bochem, A.E.; Zhang, H.; Molusky, M.M.; Wang, W.; Abramowicz, S.; la Bastide-van, G.S.; Wang, N.; et al. Cholesterol Efflux Pathways Suppress Inflammasome Activation, NETosis, and Atherogenesis. *Circulation* **2018**, *138*, 898–912. [[CrossRef](#)] [[PubMed](#)]
29. Fotakis, P.; Kothari, V.; Thomas, D.G.; Westerterp, M.; Molusky, M.M.; Altin, E.; Abramowicz, S.; Wang, N.; He, Y.; Heinecke, J.W.; et al. Anti-Inflammatory Effects of HDL (High-Density Lipoprotein) in Macrophages Predominate Over Proinflammatory Effects in Atherosclerotic Plaques. *Arterioscler. Thromb. Vasc. Biol.* **2019**, *39*, e253–e272. [[CrossRef](#)]
30. Van der Vorst, E.P.C.; Theodorou, K.; Wu, Y.; Hoeksema, M.A.; Goossens, P.; Bursill, C.A.; Aliyev, T.; Huitema, L.F.A.; Tas, S.W.; Wolfs, I.M.J.; et al. High-Density Lipoproteins Exert Pro-inflammatory Effects on Macrophages via Passive Cholesterol Depletion and PKC-NF- κ B/STAT1-IRF1 Signaling. *Cell Metab.* **2017**, *25*, 197–207. [[CrossRef](#)]
31. Dergunova, L.V.; Nosova, E.V.; Dmitrieva, V.G.; Rozhkova, A.V.; Bazaeva, E.V.; Limborska, S.A.; Dergunov, A.D. HDL cholesterol is associated with PBM expression of genes involved in HDL metabolism and atherogenesis. *J. Med. Biochem.* **2020**, *39*, 372–383. [[CrossRef](#)] [[PubMed](#)]
32. Ashburner, M.; Ball, C.A.; Blake, J.A.; Botstein, D.; Butler, H.; Cherry, J.M.; Davis, A.P.; Dolinski, K.; Dwight, S.S.; Eppig, J.T.; et al. Gene ontology: Tool for the unification of biology. The Gene Ontology Consortium. *Nat. Genet.* **2000**, *25*, 25–29. [[CrossRef](#)] [[PubMed](#)]
33. Carbon, S.; Douglass, E.; Good, B.M.; Unni, D.R.; Harris, N.L.; Mungall, C.J.; Basu, S.; Chisholm, R.L.; Dodson, R.J.; Hartline, E.; et al. The Gene Ontology resource: Enriching a GOLD mine. *Nucleic Acids Res.* **2021**, *49*, D325–D334.
34. Kanehisa, M.; Goto, S.; Kawashima, S.; Nakaya, A. The KEGG databases at GenomeNet. *Nucleic Acids Res.* **2002**, *30*, 42–46. [[CrossRef](#)]
35. Sherman, B.T.; Hao, M.; Qiu, J.; Jiao, X.; Baseler, M.W.; Lane, H.C.; Imamichi, T.; Chang, W. DAVID: A web server for functional enrichment analysis and functional annotation of gene lists (2021 update). *Nucleic Acids Res.* **2022**, *50*, W216–W221. [[CrossRef](#)]
36. Szklarczyk, D.; Gable, A.L.; Nastou, K.C.; Lyon, D.; Kirsch, R.; Pyysalo, S.; Doncheva, N.T.; Legeay, M.; Fang, T.; Bork, P.; et al. The STRING database in 2021: Customizable protein-protein networks, and functional characterization of user-uploaded gene/measurement sets. *Nucleic Acids Res* **2021**, *49*, D605–D612. [[CrossRef](#)]
37. Shannon, P.; Markiel, A.; Ozier, O.; Baliga, N.S.; Wang, J.T.; Ramage, D.; Amin, N.; Schwikowski, B.; Ideker, T. Cytoscape: A software environment for integrated models of biomolecular interaction networks. *Genome Res.* **2003**, *13*, 2498–2504. [[CrossRef](#)]
38. O'Brien, R.M. A Caution Regarding Rules of Thumb for Variance Inflation Factors. *Qual. Quant.* **2007**, *41*, 673–690. [[CrossRef](#)]
39. Pfaffl, M.W.; Horgan, G.W.; Dempfle, L. Relative expression software tool (REST) for group-wise comparison and statistical analysis of relative expression results in real-time PCR. *Nucleic Acids Res.* **2002**, *30*, e36. [[CrossRef](#)]
40. Vandesompele, J.; De, P.K.; Pattyn, F.; Poppe, B.; Van, R.N.; De, P.A.; Speleman, F. Accurate normalization of real-time quantitative RT-PCR data by geometric averaging of multiple internal control genes. *Genome Biol.* **2002**, *3*, RESEARCH0034. [[CrossRef](#)]

41. McDonald, J.H. Multiple comparisons. In *Handbook of Biological Statistics*, 3rd ed.; Sparky House Publishing: Baltimore, MD, USA, 2014; pp. 254–260. Available online: <http://www.biostathandbook.com/multiplecomparisons.html> (accessed on 14 July 2023).
42. Dergunov, A.D.; Litvinov, D.Y.; Bazaeva, E.V.; Dmitrieva, V.G.; Nosova, E.V.; Rozhkova, A.V.; Dergunova, L.V. Relation of High-Density Lipoprotein Charge Heterogeneity, Cholesterol Efflux Capacity, and the Expression of High-Density Lipoprotein-Related Genes in Mononuclear Cells to the HDL-Cholesterol Level. *Lipids* **2018**, *53*, 979–991. [[CrossRef](#)]
43. Chen, H.H.; Stewart, A.F. Transcriptomic Signature of Atherosclerosis in the Peripheral Blood: Fact or Fiction? *Curr. Atheroscler. Rep.* **2016**, *18*, 77. [[CrossRef](#)] [[PubMed](#)]
44. Liu, M.; Jiang, S.; Ma, Y.; Ma, J.; Hassan, W.; Shang, J. Peripheral-blood gene expression profiling studies for coronary artery disease and its severity in Xinjiang population in China. *Lipids Health Dis.* **2018**, *17*, 154. [[CrossRef](#)] [[PubMed](#)]
45. Wang, C.; Song, C.; Liu, Q.; Zhang, R.; Fu, R.; Wang, H.; Yin, D.; Song, W.; Zhang, H.; Dou, K. Gene Expression Analysis Suggests Immunological Changes of Peripheral Blood Monocytes in the Progression of Patients With Coronary Artery Disease. *Front. Genet.* **2021**, *12*, 641117. [[CrossRef](#)] [[PubMed](#)]
46. Miao, L.; Yin, R.X.; Huang, F.; Yang, S.; Chen, W.X.; Wu, J.Z. Integrated analysis of gene expression changes associated with coronary artery disease. *Lipids Health Dis.* **2019**, *18*, 92. [[CrossRef](#)] [[PubMed](#)]
47. Prakash, T.; Ramachandra, N.B. Integrated Network and Gene Ontology Analysis Identifies Key Genes and Pathways for Coronary Artery Diseases. *Avicenna J. Med. Biotechnol.* **2021**, *13*, 15–23. [[CrossRef](#)]
48. Byars, S.G.; Inouye, M. Genome-Wide Association Studies and Risk Scores for Coronary Artery Disease: Sex Biases. *Adv. Exp. Med. Biol.* **2018**, *1065*, 627–642.
49. Litvinov, D.Y.; Savushkin, E.V.; Dergunov, A.D. Intracellular and Plasma Membrane Events in Cholesterol Transport and Homeostasis. *J. Lipids* **2018**, *2018*, 3965054. [[CrossRef](#)]
50. Alagarsamy, J.; Jaeschke, A.; Hui, D.Y. Apolipoprotein E in Cardiometabolic and Neurological Health and Diseases. *Int. J. Mol. Sci.* **2022**, *23*, 9892. [[CrossRef](#)]
51. Ference, B.A.; Kastelein, J.J.P.; Ray, K.K.; Ginsberg, H.N.; Chapman, M.J.; Packard, C.J.; Laufs, U.; Oliver-Williams, C.; Wood, A.M.; Butterworth, A.S.; et al. Association of Triglyceride-Lowering LPL Variants and LDL-C-Lowering LDLR Variants With Risk of Coronary Heart Disease. *JAMA* **2019**, *321*, 364–373. [[CrossRef](#)]
52. Kanonidou, C. Small dense low-density lipoprotein: Analytical review. *Clin. Chim. Acta* **2021**, *520*, 172–178. [[CrossRef](#)] [[PubMed](#)]
53. Seo, T.; Al-Haideri, M.; Treskova, E.; Worgall, T.S.; Kako, Y.; Goldberg, I.J.; Deckelbaum, R.J. Lipoprotein lipase-mediated selective uptake from low density lipoprotein requires cell surface proteoglycans and is independent of scavenger receptor class B type 1. *J. Biol. Chem.* **2000**, *275*, 30355–30362. [[CrossRef](#)]
54. Bayly, G.R. Lipids and Disorders of Lipoprotein Metabolism. In *Clinical Biochemistry: Metabolic and Clinical Aspects Chapter 37*, 3rd ed.; Marshall, W.J., Lapsley, M., Day, A.P., Ayling, R.M., Eds.; Elsevier: Amsterdam, The Netherlands, 2014; pp. 702–736.
55. Goulopoulou, S.; McCarthy, C.G.; Webb, R.C. Toll-like Receptors in the Vascular System: Sensing the Dangers Within. *Pharmacol. Rev.* **2016**, *68*, 142–167. [[CrossRef](#)]
56. Lu, X.; Wang, Z.; Ye, D.; Feng, Y.; Liu, M.; Xu, Y.; Wang, M.; Zhang, J.; Liu, J.; Zhao, M.; et al. The Role of CXC Chemokines in Cardiovascular Diseases. *Front. Pharmacol.* **2021**, *12*, 765768. [[CrossRef](#)] [[PubMed](#)]
57. Beaulieu, L.M.; Lin, E.; Mick, E.; Koupenova, M.; Weinberg, E.O.; Kramer, C.D.; Genco, C.A.; Tanriverdi, K.; Larson, M.G.; Benjamin, E.J.; et al. Interleukin 1 receptor 1 and interleukin 1b regulate megakaryocyte maturation, platelet activation, and transcript profile during inflammation in mice and humans. *Arterioscler. Thromb. Vasc. Biol.* **2014**, *34*, 552–564. [[CrossRef](#)] [[PubMed](#)]
58. Rogacev, K.S.; Zawada, A.M.; Emrich, I.; Seiler, S.; Bohm, M.; Fliser, D.; Woollard, K.J.; Heine, G.H. Lower Apo A-I and lower HDL-C levels are associated with higher intermediate CD14⁺⁺CD16⁺ monocyte counts that predict cardiovascular events in chronic kidney disease. *Arterioscler. Thromb. Vasc. Biol.* **2014**, *34*, 2120–2127. [[CrossRef](#)] [[PubMed](#)]
59. Schnabel, R.B.; Yin, X.; Larson, M.G.; Yamamoto, J.F.; Fontes, J.D.; Kathiresan, S.; Rong, J.; Levy, D.; Keaney, J.F., Jr.; Wang, T.J.; et al. Multiple inflammatory biomarkers in relation to cardiovascular events and mortality in the community. *Arterioscler. Thromb. Vasc. Biol.* **2013**, *33*, 1728–1733. [[CrossRef](#)]
60. Xiao, X.; Yang, C.; Qu, S.L.; Shao, Y.D.; Zhou, C.Y.; Chao, R.; Huang, L.; Zhang, C. S100 proteins in atherosclerosis. *Clin. Chim. Acta* **2020**, *502*, 293–304. [[CrossRef](#)]
61. Xiao, S.; Kuang, C. Identification of crucial genes that induce coronary atherosclerosis through endothelial cell dysfunction in AMI-identifying hub genes by WGCNA. *Am. J. Transl. Res.* **2022**, *14*, 8166–8174.
62. Antonov, A.S.; Kolodgie, F.D.; Munn, D.H.; Gerrity, R.G. Regulation of macrophage foam cell formation by alphaVbeta3 integrin: Potential role in human atherosclerosis. *Am. J. Pathol.* **2004**, *165*, 247–258. [[CrossRef](#)]
63. Schneider, J.G.; Zhu, Y.; Coleman, T.; Semenkovich, C.F. Macrophage beta3 integrin suppresses hyperlipidemia-induced inflammation by modulating TNFalpha expression. *Arterioscler. Thromb. Vasc. Biol.* **2007**, *27*, 2699–2706. [[CrossRef](#)] [[PubMed](#)]
64. Dergunov, A.D.; Ponthieux, A.; Mel'kin, M.V.; Lambert, D.; Sokolova, O.Y.; Akhmedzhanov, N.M.; Visvikis-Siest, S.; Siest, G. Capillary isotachopheresis study of lipoprotein network sensitive to apolipoprotein E phenotype. 2. ApoE and apoC-III relations in triglyceride clearance. *Mol. Cell. Biochem.* **2009**, *325*, 25–40. [[CrossRef](#)]
65. Manchev, V.T.; Hilpert, M.; Berrou, E.; Elaib, Z.; Aouba, A.; Boukour, S.; Souquere, S.; Pierron, G.; Rameau, P.; Andrews, R.; et al. A new form of macrothrombocytopenia induced by a germ-line mutation in the PRKACG gene. *Blood* **2014**, *124*, 2554–2563. [[CrossRef](#)]

66. Moen, L.V.; Sener, Z.; Volchenkov, R.; Svarstad, A.C.; Eriksen, A.M.; Holen, H.L.; Skalhegg, B.S. Ablation of the Cbeta2 subunit of PKA in immune cells leads to increased susceptibility to systemic inflammation in mice. *Eur. J. Immunol.* **2017**, *47*, 1880–1889. [[CrossRef](#)] [[PubMed](#)]
67. Wang, R.; Xu, J.; Tang, Y.; Wang, Y.; Zhao, J.; Ding, L.; Peng, Y.; Zhang, Z. Transcriptome-wide analysis reveals the coregulation of RNA-binding proteins and alternative splicing genes in the development of atherosclerosis. *Sci. Rep.* **2023**, *13*, 1764. [[CrossRef](#)]
68. Raghavan, S.; Singh, N.K.; Gali, S.; Mani, A.M.; Rao, G.N. Protein Kinase C theta Via Activating Transcription Factor 2-Mediated CD36 Expression and Foam Cell Formation of Ly6C(hi) Cells Contributes to Atherosclerosis. *Circulation* **2018**, *138*, 2395–2412. [[CrossRef](#)] [[PubMed](#)]

Disclaimer/Publisher's Note: The statements, opinions and data contained in all publications are solely those of the individual author(s) and contributor(s) and not of MDPI and/or the editor(s). MDPI and/or the editor(s) disclaim responsibility for any injury to people or property resulting from any ideas, methods, instructions or products referred to in the content.